

Ajam, H and Lastra-Gonzalez, P and Gomez-Meijide, B and Airey, Gordon and Garcia, Alvaro (2017) Self-Healing of Dense Asphalt Concrete by Two Different Approaches: Electromagnetic Induction and Infrared Radiation. *Journal of Testing and Evaluation*, 45 (6). pp. 1933-1940. ISSN 1945-7553

**Access from the University of Nottingham repository:**

<http://eprints.nottingham.ac.uk/50789/1/JTE20160612.R1.pdf>

**Copyright and reuse:**

The Nottingham ePrints service makes this work by researchers of the University of Nottingham available open access under the following conditions.

This article is made available under the University of Nottingham End User licence and may be reused according to the conditions of the licence. For more details see:

[http://eprints.nottingham.ac.uk/end\\_user\\_agreement.pdf](http://eprints.nottingham.ac.uk/end_user_agreement.pdf)

**A note on versions:**

The version presented here may differ from the published version or from the version of record. If you wish to cite this item you are advised to consult the publisher's version. Please see the repository url above for details on accessing the published version and note that access may require a subscription.

For more information, please contact [eprints@nottingham.ac.uk](mailto:eprints@nottingham.ac.uk)



ASTM INTERNATIONAL

# REPRINTS ORDER FORM

For reprints of articles and/or papers from ASTM Journals, Selected Technical Papers (STPs), book chapters and *Standardization News*.

**NOTE:** Authors receive a 25% discount

**SHIP To:**

Name: \_\_\_\_\_

Organization: \_\_\_\_\_

Address: \_\_\_\_\_

City: \_\_\_\_\_ State: \_\_\_\_\_ Zip: \_\_\_\_\_

Country: \_\_\_\_\_

**BILL To:**

Name: \_\_\_\_\_

Organization: \_\_\_\_\_

Address: \_\_\_\_\_

City: \_\_\_\_\_ State: \_\_\_\_\_ Zip: \_\_\_\_\_

Country: \_\_\_\_\_

Date:

Phone:

email:

Fax:

**Paper Title:** \_\_\_\_\_

**Publication:** \_\_\_\_\_  
(Title, month, and volume number; STP number; or stock number)

**Page length of article:** \_\_\_\_\_ **Number of copies:** (25 copies minimum) \_\_\_\_\_

**Cover:** (check one)

Reprinted article, no cover

Reprinted article and cover with typeset title of article and author's name

**QUESTIONS ABOUT YOUR ORDER?**

Call Customer Relations at 610/832-9585, weekdays 8:30am-4:30pm ET

**COMPLETE QUOTE REQUEST AND RETURN TO:**

- 1. SERVICE@ASTM.ORG
- 2. FAX: 610/832-9555
- 3. MAIL TO:

**CUSTOMER RELATIONS**  
*ASTM International* Customer Service  
100 Barr Harbor Drive  
West Conshohocken, PA 19428-2959



ASTM INTERNATIONAL

# REPRINTS PRICE SCALE\*

## COLOR REPRINTS

Copies Pages	100	200	500	1000	2000
2	\$1,102	\$1,323	\$1,543	\$1,764	\$1,984
3-4	\$2,116	\$2,221	\$2,326	\$2,425	\$2,824
5-8	\$2,168	\$2,278	\$2,394	\$2,499	\$3,024
9-12	\$3,307	\$3,470	\$3,638	\$3,801	\$4,126


## BLACK & WHITE REPRINTS

Copies Pages	25	50	100	200	300	500	1000	2000
1-4	\$136	\$152	\$168	\$184	\$199	\$226	\$310	\$472
5-8	\$195	\$226	\$257	\$278	\$299	\$352	\$499	\$709
9-12	\$225	\$257	\$289	\$336	\$357	\$425	\$577	\$787
13-16	\$263	\$294	\$325	\$394	\$430	\$520	\$751	\$1,118
17-20	\$278	\$336	\$394	\$472	\$514	\$635	\$887	\$1,307
21-24	\$301	\$373	\$446	\$535	\$583	\$724	\$1,003	\$1,475
25-28	\$331	\$404	\$478	\$583	\$646	\$808	\$1,165	\$1,795
29-32	\$383	\$441	\$499	\$651	\$724	\$913	\$1,323	\$2,058
Cover (optional)	\$100	\$115	\$136	\$157	\$178	\$220	\$373	\$598

\* Prices are subject to change without notice.

ASTM International Customer Relations department will finalize your reprint quote including freight charges. ASTM International will contact you with the quote price.

## AUTHOR QUERY FORM

 ASTM INTERNATIONAL	<b>Journal: J. Test. Eval.</b>  <b>Article Number: JTE20160612</b>	<p>Please provide your responses and any corrections by annotating this PDF and uploading it to ASTM's eProof website as detailed in the Welcome email.</p>
---	--	---

Dear Author,

Below are the queries associated with your article; please answer all of these queries before sending the proof back to Cenveo. Author please indicate the correct color processing option from the list below:

1. Author, please confirm Figure number(s) that should appear as color in print. Please know that any associated mandatory fees will apply for figures printed in color.
2. Author, please confirm Figure number(s) that should appear as color online only, there will be no fees applied.
3. Please note the use of color in your figures may not be clear to the reader once converted to black and white for print. Please review your figure(s) carefully and make adjustments as necessary. Please confirm if your figure is acceptable to print in B/W. If necessary, please provide revised figures.
4. Author, your paper currently does not include any color figures for online or print. If color is needed please indicate which figures it should be applied to and whether it is color in print or online.

Location in article	Query / Remark: click on the Q link to navigate to the appropriate spot in the proof. There, insert your comments as a PDF annotation.
<a href="#">AQ1</a>	Please provide postal mailing addresses for all authors; authors for whom we receive a complete address will receive one complimentary copy of the issue.
<a href="#">AQ2</a>	Please verify email address.
<a href="#">AQ3</a>	Please note that equation 11 was previously numbered 9. Please check that equation citation numbers in the text match the correct equations.
<a href="#">AQ4</a>	Note that figures are black and white in print. Please confirm that Figure 9 and 10 will be understandable to readers of the print version.
<a href="#">AQ5</a>	ASTM journals now require archived URLs for all references that include URLs. To archive a website, copy its URL, go to <a href="http://www.web.archive.org">www.web.archive.org</a> , and paste the URL into the box in the lower right corner that says "Save Page Now". You will then receive a new (archived) URL. This is the URL that must be included in your reference list, along with the day, month, and year of access. Please see the ASTM Instructions for Authors for more information.
<a href="#">AQ6</a>	Please provide issue number for reference 2, 3, 5, 6, 8, 9, 11, 12, 15, 18, 21.

Thank you for your assistance.



# Journal of Testing and Evaluation

---

H. Ajam,<sup>1</sup> P. Lastra-González,<sup>2</sup> B. Gómez-Meijide,<sup>1</sup> G. Airey,<sup>3</sup> and A. Garcia<sup>1</sup>

**DOI: 10.1520/JTE20160612**

Author Proof

## Self-Healing of Dense Asphalt Concrete by Two Different Approaches: Electromagnetic Induction and Infrared Radiation

---

VOL. 45 / NO. 6 / NOVEMBER 2017



H. Ajam,<sup>1</sup> P. Lastra-González,<sup>2</sup> B. Gómez-Meijide,<sup>1</sup> G. Airey,<sup>3</sup> and A. Garcia<sup>1</sup>

1 AQ1

# Self-Healing of Dense Asphalt Concrete by Two Different Approaches: Electromagnetic Induction and Infrared Radiation

## Reference

Ajam, H., Lastra-González, P., Gómez-Meijide, B., Airey, G., and Garcia, A., "Self-Healing of Dense Asphalt Concrete by Two Different Approaches: Electromagnetic Induction and Infrared Radiation," *Journal of Testing and Evaluation*, Vol. 45, No. 6, 2017, pp. 1-8, <http://dx.doi.org/10.1520/JTE20160612>. ISSN 0090-3973

## ABSTRACT

Self-healing of cracks in asphalt mixtures is a phenomenon that can be accelerated by reducing the viscosity of bitumen as it increases the capillarity flow through the cracks. One method to achieve this is by increasing temperature, which also produces a thermal expansion that contributes to the circulation of the bitumen through cracks. In the present paper, the healing performance of asphalt mixture heated using infrared heating to simulate the natural solar radiation, and induction heating, a new method to increase the temperature of asphalt pavements, were compared in terms of time and healing temperature. Healing was defined as the relationship between the 3-point bending strength of an asphalt beam before and after healing. The results show that both methods reach similar and satisfactory healing ratios at around 90 %. However, induction heating is more energy efficient because the effect is concentrated on the binder, instead of heating the whole mix. This can be translated into much shorter heating times to reach the same healing level. Finally, an optimum radiation energy was found, after which higher amounts of infrared radiation damage the properties of the healed material.

## Keywords

self-healing, induction heating, infrared radiation, asphalt materials

Manuscript received November 25, 2016; accepted for publication March 8, 2017; published online xx xx xxxx.

<sup>1</sup> Nottingham Transportation Engineering Centre [NTEC], Dept. of Civil Engineering, Univ. of Nottingham, Nottingham NG7 2RD, UK

<sup>2</sup> GITECO Research Group, Universidad de Cantabria. E.T.S. Ingenieros de Caminos, Canales y Puertos de Santander, Av. de los Castros s/n, 39005 Santander, Spain

<sup>3</sup> Nottingham Transportation Engineering Centre [NTEC], Dept. of Civil Engineering, Univ. of Nottingham, Nottingham NG7 2RD, UK (Corresponding author), e-mail: [gordon.airey@nottingham.ac.uk](mailto:gordon.airey@nottingham.ac.uk)  
 <http://orcid.org/0000-0002-2891-2517>

AQ2

## 18 Introduction

19 Aggregate particles in asphalt materials are bonded together by  
20 asphalt bitumen, a complex visco-elasto-plastic liquid whose  
21 rheological properties, including the viscosity, depend to a great  
22 degree on its temperature [1]. When the temperature exceeds a  
23 critical value, so-called Newtonian temperature, bitumen starts  
24 flowing throughout the pores and capillaries of the material in  
25 an accelerated manner [2]. Under the same principle, micro-  
26 cracks produced in asphalt roads by traffic, weather exposure,  
27 etc. [3] can be quickly healed by simply increasing the tempera-  
28 ture above the Newtonian temperature of the material [4], being  
29 the process more effective as the temperature increases [5].

30 To put this into practice, one of the most promising  
31 approaches is using induction heating technology [6,7], which  
32 involves the previous addition of electrically conductive fibers  
33 [8] or powder [9] into the asphalt mixture. When a given road  
34 contains these kinds of particles, they can be heated by  
35 simply applying an external varying electromagnetic field,  
36 which induces micro-currents and heats the particles through  
37 the Joule's effect [10]. The healing level that can be achieved by  
38 this method depends on the diameter, material composition,  
39 and length of the fibers [11]; it can also be predicted through  
40 the model proposed by Garcia et al. [12] based on the equilib-  
41 rium of surface tension, gravity, and dissipation forces caused  
42 by the movement of bitumen against the walls of the crack.

43 It is also known that, besides the temperature, asphalt self-  
44 healing is mainly affected by intrinsic properties of the material,  
45 such as the viscosity [13] and chemical composition [14] of  
46 bitumen, type of aggregates [15], and compaction level of the  
47 mix [16]. However, roads placed in hot environments that are  
48 exposed for long times to temperatures higher than 70°C [17]  
49 are not perpetually healed. Instead, the cracks form and grow  
50 until some form of maintenance is required.

51 Throughout the present investigation, a comparison  
52 between the healing dynamics produced by electromagnetic  
53 induction and solar radiation (simulated by means of infrared  
54 lamps) was carried out to find answers to these questions and to

55 assess the effectiveness and energy efficiency of induction heat-  
56 ing compared to the natural process of solar radiation. To  
57 obtain this, dense asphalt beams were manufactured containing  
58 steel grit as healing agents, and 3-point bending strength was  
59 tested before and after applying either an induction or infrared  
60 treatment on cracked samples. To compare both methods in a  
61 fair way, the concept of healing energy described by Gómez-  
62 Meijide et al. [18] was applied. Finally, the rheology of bitumen  
63 samples subjected to different radiation times was assessed to  
64 see to what extent the material aging affects the self-healing  
65 properties of asphalt materials.

## 66 Materials and Methods

### 67 DESCRIPTION OF MATERIALS

68 The asphalt samples used during the present investigation for  
69 the healing tests were produced with continuous and dense  
70 aggregate gradation with a target void content of 4.5 % (Fig. 1).  
71 The natural aggregate was limestone, whereas the conductive  
72 component was a metal grit with uniformed size of 1 mm. The  
73 latter was introduced into the mix by replacing part of the natu-  
74 ral aggregate in this fraction. The volumetric content of metal  
75 grit in the mix was fixed at 4 % (11.2 % by weight). The selected  
76 binder was a 40/60 pen and the content was 4.7 %.

### 77 TEST SPECIMEN PREPARATION

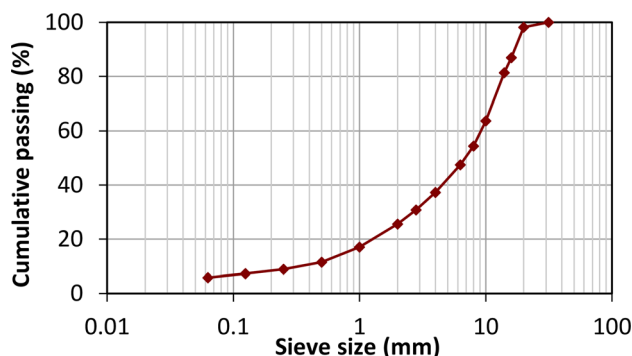
78 The gradation was batched by blending samples of limestone  
79 with different gradations together with the metal grit. The  
80 asphalt concrete was mixed in a laboratory mixer at 160°C for  
81 2 min, and then compacted as slabs by means of roller compac-  
82 tor until it reached the target void content of 4.5 %. The dimen-  
83 sions of the slabs were 310 × 310 × 50 mm<sup>3</sup>. Then, the slabs  
84 were cut by a radial saw blade suitable for concrete and stone  
85 materials, obtaining eight 150 × 70 × 50 mm<sup>3</sup> prismatic samples  
86 from each slab. To see how this process affected the samples,  
87 the air void content was measured for a series of six samples,  
88 obtaining an average value of 4.70 % and a standard deviation  
89 of 0.56 %. Finally, a notch was cut at the midpoint from the cen-  
90 tral axis of the beams, with a thickness of about 2 mm and a  
91 depth of about 10 mm (Fig. 2).

### 92 TESTING OF ASPHALT SELF-HEALING

93 Although other possible characteristics in the non-destructive  
94 zone (e.g., recovery of stiffness or viscosity) were considered to  
95 study the self-healing capacity of the material, the present study  
96 was eventually carried out through the strength recovery on  
97 complete and brittle cracks (splitting the samples in two halves)  
98 to tests them under the most similar conditions possible (same  
99 crack area, position, etc.).

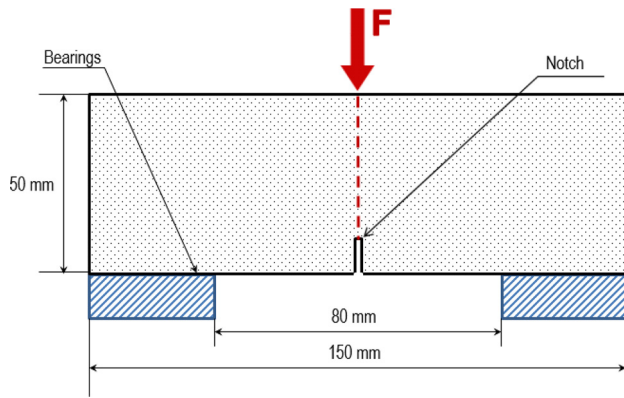
100 The samples were first tested under 3-point bending at  
101 -20°C to obtain a brittle and clean crack, while minimizing the  
102 effect of permanent deformations. The tests were carried out

FIG. 1 Aggregate gradation used for the present investigation.





**FIG. 2** Design of the 3-point bending test to break the samples.



103 under strain-controlled conditions, with an increasing load  
 104 ramp at a deformation rate of 0.5 mm/min. During each test, a  
 105 clear crack of approximately 200 μm width was produced, cross-  
 106 ing vertically through the samples, from the notch to the load  
 107 application point (Fig. 2).

108 Once the crack was produced and the sample was split in  
 109 two different halves, they were put together again and healed by  
 110 means of one of the following methods:

- 112 (1) Induction heating: The samples were exposed to induc-  
 113 tion heating for 19 different times between 15 s and  
 114 240 s. No times longer than 240 s were used as the bitu-  
 115 men reached its burning temperature. The distance from  
 116 the upper side of the sample to the coil was 1.5 cm, the  
 117 current 80 A, frequency 348 kHz, and the power used  
 118 2800 W (Fig. 3, left).
- 120 (2) Infrared radiation: To simulate the effect of the sun  
 121 under controlled and steady conditions of temperature  
 122 and radiation level over the whole testing time, the sam-  
 123 ples were placed under four infrared lamps at a distance  
 124 of 30 cm. The samples were embedded in white porous  
 125 sand (Catsan cat litter) with the exception of the upper

side to prevent them receiving infrared radiation 126  
 from any other side and to avoid the deformation caused 127  
 by high temperatures (Fig. 3, right). The samples were 128  
 exposed to infrared heating for 42 different times 129  
 between 5 min and 5760 min (96 h). 130

The temperature of the samples was constantly monitored 131  
 by using an infrared camera for asphalt induction heating and 132  
 thermocouples installed on the top and the bottom of the test 133  
 specimens in the case of infrared heating. 134

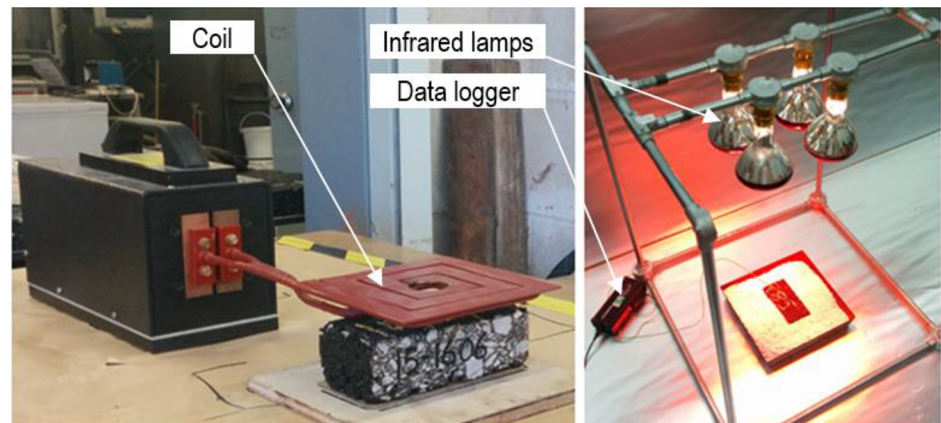
Once the healing process was finished, the samples were 135  
 cooled at -20°C and tested again under 3-point bending. The 136  
 healing ratio (*S*) of asphalt samples was defined as the relation- 137  
 ship between the ultimate force resisted by the test specimens 138  
 during a 3-point bending test before being split into two halves, 139  
 $F_b$ , and the ultimate force measured for the same specimen and 140  
 under the same conditions but when repeating the test after the 141  
 healing process  $F_b'$ : 142

$$S(\tau) = \frac{F_b(\tau)}{F_i} \quad (1)$$

**BITUMEN RHEOLOGY** 143

Bitumen aging produced during the healing processes was stud- 144  
 ied by recovering, by rotary evaporator, the bitumen from five 145  
 compacted samples of dense asphalt mix exposed to infrared 146  
 radiation for 0 min, 200 min, 1 day, 2 days, and 4 days. The 147  
 rheology of bitumen was examined using a dynamic shear rhe- 148  
 ometer (Bohlin Gemini HR nano), configured with 25-mm- 149  
 diameter parallel plates with a gap between them of 1 mm. The 150  
 range of oscillatory frequencies was between 0.1 Hz and 10 Hz 151  
 and temperatures between 30°C and 70°C (at 5°C intervals). 152  
 Constant strain of 1 % was fixed to ensure the linear viscoelastic 153  
 behavior of the samples; complex viscosity ( $\eta^*$ ) and complex 154  
 modulus ( $G^*$ ) were obtained for each frequency and 155  
 temperature. 156

**FIG. 3** Healing procedures by induction heating (left) and infrared radiation (right).





157 The corresponding curves of  $G^*$  versus frequency, obtained  
 158 at different temperatures can be merged into a single smooth  
 159 function by applying the principle of time-temperature super-  
 160 position [19]. In the present investigation, the resulting master  
 161 curves were constructed by fixing a reference temperature of  
 162 30°C and shifting the rest of the data by means of a shift factor.  
 163 As a result, the complex modulus was mathematically modeled  
 164 as the following sigmoidal function [20]:

$$\log|G^*| = \delta + \frac{\alpha}{1 + e^{\beta + \gamma(\log t_r)}} \quad (2)$$

165 where:

166  $t_r$  = the reduced time of loading at the reference  
 167 temperature,

168  $\delta$  = the minimum value of  $G^*$ ,

169 the sum  $\delta + \alpha$  = the maximum value of  $G^*$ , and

170 the parameters  $\beta$  and  $\gamma$  = the shape of the sigmoidal  
 171 function.

172 Data shifting is made by using a shift factor, whose form  
 173 for a certain temperature of interest ( $T$ ) is:

$$a(t) = \frac{t}{t_r} \quad (3)$$

174 where:

175  $t$  = the time of loading at the desired temperature, and

176  $t_r$  = the reduced time of loading at the reference  
 177 temperature.

## 178 Theoretical Framework

179 Asphalt self-healing does not happen only during the heating  
 180 periods, but also during cooling [2]. The analytical relationship  
 181 between time and temperature can be obtained for heating and  
 182 cooling stages by integrating Newton's law of heat transfer:

$$mc \frac{dT}{dt} = -kA(T - T_c) \quad (4)$$

183 where:

184  $k$  = a heat transfer coefficient ( $s^{-1}$ ), which depends of the  
 185 area of the beams exposed to the environment, mass of the test  
 186 samples, and specific heat capacity,

187  $T$  (K) = the temperature of the sample,

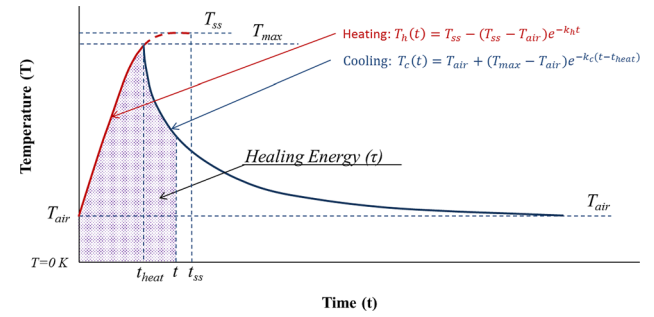
188  $T_c$  (K) = a fixed temperature to which the sample tempera-  
 189 ture tends and that can be the ambient temperature ( $T_{air}$ )  
 190 during cooling or the steady-state temperature reached by the  
 191 sample during heating ( $T_{ss}$ ),

192  $m$  (g) = the mass of the sample, and

193  $c$  (J/g °C) = the specific heat.

194 In Ref 18, the expressions of both heating and cooling  
 195 curves were obtained (Fig. 4). In addition, the concept of healing  
 196 energy was also developed in Ref 18 as the total area below the

FIG. 4 Healing energy as the area below the heating and cooling curves.



197 curves. Thus, considering a cooling process of 4 h at ambient  
 198 temperature, this parameter (in K·s) can be calculated as:

$$\tau(t) = \tau_h(t_{heat}) + \tau_c(4h) \quad (5)$$

199 where:

$$\tau_h(t) = T_{ss} + \frac{T_{ss} - T_{air}}{k_h} (e^{-k_h t} - 1); \quad t < t_{heat} \quad (6)$$

$$\tau_c(t) = T_{air} \cdot (t - t_{heat}) + \frac{T_{max} - T_{air}}{k_c} (1 - e^{-k_c(t - t_{heat})}); \quad t > t_{heat} \quad (7)$$

200 where:

201  $T_{air}$  = the ambient temperature,

202  $T_{ss}$  = the steady-state temperature reached by asphalt mix-  
 203 ture during heating, and

204  $t_{heat}$  = the heating time of the test sample.

205 As the heating and cooling rates may differ during the heat-  
 206 ing and cooling periods, the heat transfer coefficient has been  
 207 noted as  $k_h$  for the heating period and  $k_c$  for the cooling  
 208 period. Both can be obtained by fitting the experimental  
 209 temperature-time curves to these equations.

210 In addition, in Ref 2, a predictive model for the healing of  
 211 asphalt materials was defined as follows:

$$S(\tau) = \frac{C_1}{F_0} \cdot e^{-D\tau} \left( -1 + e^{\frac{D\tau}{2}} \right)^2 \quad (8)$$

212 where:

213  $S(\tau)$  = the healing ratio or percentage of recovered strength  
 214 after the healing treatment (%),

215  $F_0$  = the initial 3-point bending strength of the test samples  
 216 (kN),

217  $\tau$  = the healing energy explained above (K·s), and

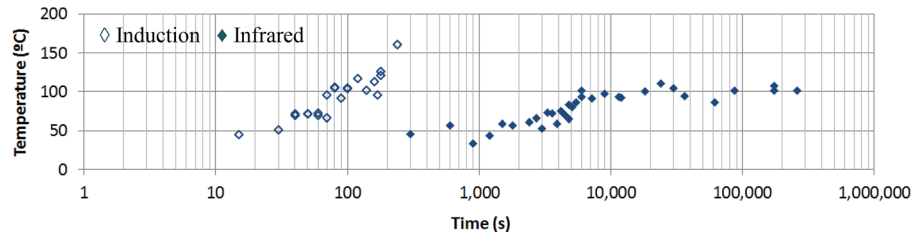
218  $D$  and  $C_1$  = parameters that can be calculated as:

$$D = \frac{\rho g r}{\beta} \quad (9)$$

$$C_1 = 8 \frac{\sigma_u \cdot C}{L \cdot H} \quad (10)$$

**FIG. 5**

Maximum temperature (°C) reached by the samples after different healing times.



219 where:

- 220  $\rho$  = the density of material ( $\text{kg/m}^3$ ),
- 221  $g$  = the gravity ( $\text{m/s}^2$ ),
- 222  $r$  = the width of the crack (m),
- 223  $\beta$  = a dimensionless parameter that takes into account
- 224 possible sources of energy losses,
- 225  $\sigma_u$  = the maximum force resisted by the beam (N),
- 226  $L$  = the span of the beam (m),
- 227  $H$  = its height, and
- 228  $C$  = a material constant with units ( $\text{m}^2$ ).

229 Finally, the effect of aging was not introduced in these  
 230 equations, as it was assumed that, for the temperatures and  
 231 times used in the tests, it would produce low impact in the heal-  
 232 ing performance of the mix (i.e., mixes heated by induction  
 233 reach high temperature but just for seconds, whereas the infra-  
 234 red radiation affects, especially, the superficial part of the speci-  
 235 mens). The low affection of aging in the healing results could be  
 236 checked by the rheology tests, as described in the next section.

## 237 Results

238 **Fig. 5** shows the temperature reached by the samples depending  
 239 on the heating time. As can be seen, infrared heating is a much  
 240 slower method than induction heating. As an example, the sam-  
 241 ples subjected to induction reached the temperature of  $80^\circ\text{C}$  in  
 242 1 min, whereas by infrared heating it took around 85 min to  
 243 reach the same temperature. This can be attributed to the fact  
 244 that induction heats only the metal grit by the Joule principle  
 245 and is very fast, whereas infrared radiation progressively heats  
 246 the whole sample by diffusion, transmitting a great part of  
 247 the heating energy to the environment. Moreover, induction

248 heating is more effective, because the temperatures that can be  
 249 reached are higher. In the case of infrared radiation, a steady-  
 250 state temperature of  $101^\circ\text{C}$  was never exceeded, whereas in the  
 251 case of induction heating the temperature never stopped grow-  
 252 ing with the heating time (the maximum heating was carried  
 253 out to 240 s because longer times produced smoke and tempera-  
 254 tures close to the flashpoint of bitumen).

255 The healing ratios obtained can be seen in **Fig. 6** (depending  
 256 on the maximum temperature reached by the samples) and  
 257 **Fig. 7** (depending on the healing time). First, it is noticeable that  
 258 both methods can reach similar and satisfactory healing ratios,  
 259 around 90 %. Furthermore, for equal maximum temperatures,  
 260 infrared radiation produced higher healing ratios. However, it  
 261 can also be seen that the amount of time necessary to reach  
 262 these values is much higher when using infrared radiation. For  
 263 example, a healing ratio of 80 % was achieved after 160 s of  
 264 induction heating (less than 3 min) and 190 min of infrared  
 265 heating. Again, this is explained through the potential of elec-  
 266 tromagnetic induction to concentrate the heating energy only in  
 267 the metal particles and the bitumen embedding them, whereas a  
 268 large part of infrared energy is wasted by heating non-healing  
 269 components, such as the aggregates, or simply being lost to the  
 270 environment.

271 Moreover, the healing ratios of the induction method never  
 272 stopped increasing with time and temperature (as the longest  
 273 induction heating test only lasted 240 s), whereas with infrared  
 274 radiation the healing ratios increased only until they reached  
 275 the steady-state temperature of  $101^\circ\text{C}$  (in 11,000–12,000 s), but  
 276 from this moment on, the healing ratios reduced again to values  
 277 close to 50 %. Therefore, although both temperature and time  
 278 affect the healing, they do it in different ways: Temperature

**FIG. 6**

Relationship between healing ratios (%) and max temperature reached by samples.

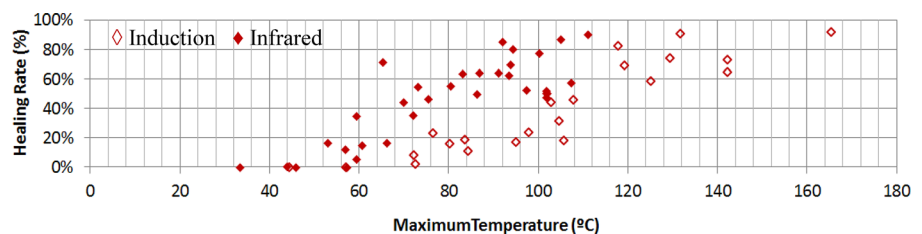
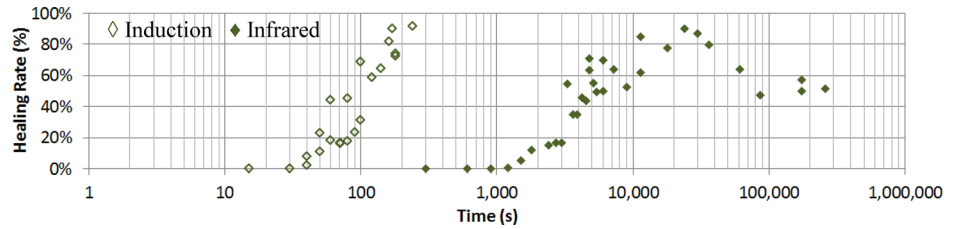


**FIG. 7**

Relationship between healing ratios (%) and healing time with different methods.



279 increases can always be translated into healing improvements.  
 280 However, maintaining a steady temperature for longer times  
 281 produces a detrimental effect on the healing. This behavior  
 282 explains why roads exposed almost every day to sunlight and  
 283 high temperatures (for instance, in desert climates) are not per-  
 284 petually healed. Instead, there exists an optimal radiation point  
 285 for asphalt self-healing. Once overcome, further radiation pro-  
 286 duces nothing but damage in the material.

287 To better understand this process, the input temperature  
 288 and time were translated into healing energy (Eqs 5–7) and  
 289 the healing model described in Eqs 8 to 10 was fitted to the  
 290 experimental data. As can be seen in Fig. 8, the model pro-  
 291 vides an excellent fit during the increasing stage of the curves  
 292 but it cannot predict the decreasing part. Because this model  
 293 is based on equilibrium of surface tension, hydrostatic forces,  
 294 and energy dissipation caused by friction, there must be at  
 295 least another factor, different from these that affects asphalt  
 296 self-healing.

297 In Fig. 8, it can also be seen that in terms of healing energy,  
 298 a critical value exists, common for both methods that triggers  
 299 the healing processes. However, after this point, the induction  
 300 heating again resulted in a more efficient method, because it  
 301 reaches higher healing levels with less energy.

302 The authors have found that a reason for the decrease of  
 303 healing levels after reaching the steady-state temperature might  
 304 be because of the aging of bitumen. To examine this, bitumen  
 305 was extracted from test specimens exposed to infrared after  
 306 0 min, 200 min, 1 day, 2 days, and 4 days, and the rheology

and flow behavior index ( $n$ ) (see Ref 21) were compared. The  
 distance between the sample and the infrared lamps was set at  
 30 cm.

In previous research [11], it was described that the healing  
 processes can only occur as long as the temperature of the  
 material remains higher than a certain threshold defined as the  
 Newtonian temperature of bitumen ( $T_{newt}$ ). This critical tem-  
 perature can be experimentally obtained through rheological  
 tests and taking into account the following power law relation-  
 ship [22]:

$$\eta^* = m \cdot |\omega|^{n-1} \quad (11)$$

where:

$\omega$  = the frequency,

$\eta^*$  = the complex viscosity, and

$m$  and  $n$  = fitting parameters ( $n$  is known as the flow behav-  
 ior index).

According to Ref 21, the behavior of the bitumen can be  
 considered near-Newtonian when  $0.9 \leq n < 1$ . The correlation  
 between  $n$  and the temperature can be seen in Fig. 9 and the  
 master curves in Fig. 10 for samples of bitumen extracted from  
 dense asphalt specimens subjected to infrared radiation of  
 lamps situated at 30 cm above the samples and over periods of  
 0 min (control), 200 min (optimum healing results for dense  
 mixtures at 30 cm) and 1, 2, and 4 days to analyze samples asso-  
 ciated with the decreasing part of the healing curve (as seen in  
 Fig. 8).

**FIG. 8**

Fitting of healing model to experimental data of healing by induction and infrared heating.

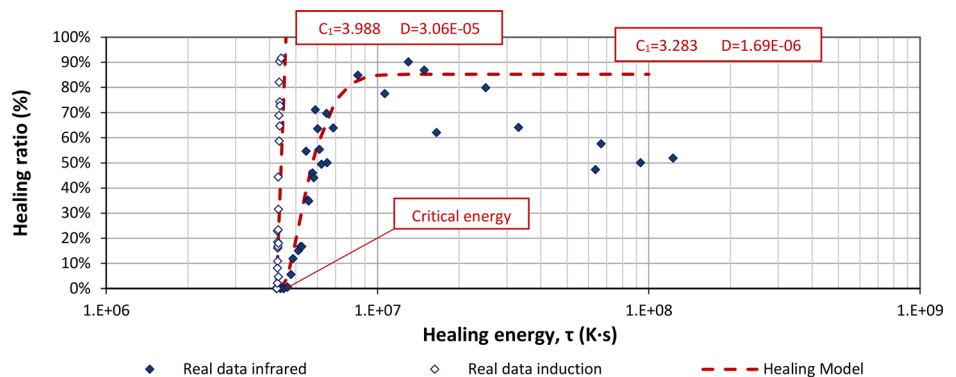
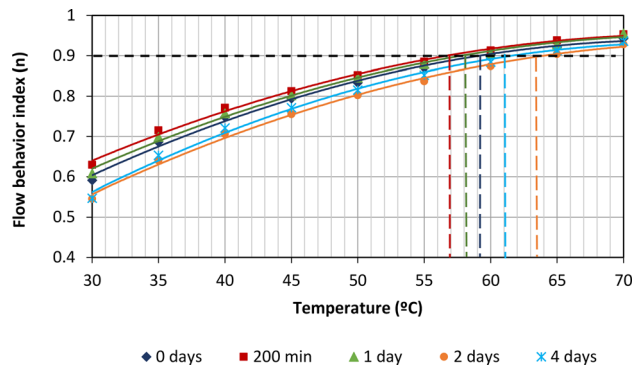


**FIG. 9** Flow behavior index ( $n$ ) of bitumen recovered from samples subjected to infrared radiation over different periods of time.



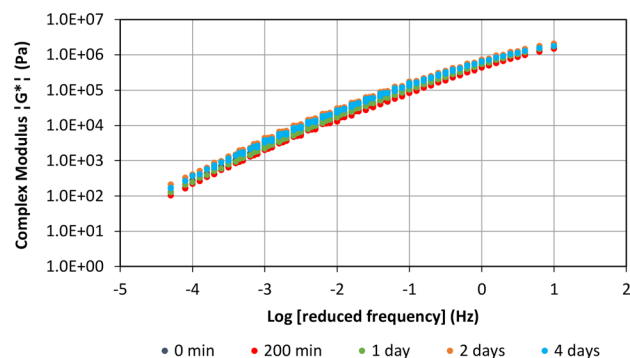
332 The results show that the rheological behavior of all the  
 333 samples is very similar, not following a clear trend with the  
 334 variations in the radiation time, and demonstrating values of  
 335 Newtonian temperature that are significantly similar. All the  
 336  $T_{newt}$ -values ranked between 56.5°C and 64.0°C (average  
 337 59.8°C). Hence, although long-term factors that can affect the  
 338 healing, such as traffic or aging in desert climates (which might  
 339 result in stiffening of asphalt and increased cracking potential),  
 340 the change of rheological properties caused by the infrared radi-  
 341 ation cannot be considered as a substantial reason to explain  
 342 the decreasing results obtained for the tested radiation times.

### 343 Conclusions

344 In the present experimental investigation, a comparison  
 345 between two different methods to induce self-healing in asphalt  
 346 mixture, induction, and infrared heating was performed. Fur-  
 347 thermore, energy and healing models from previous research  
 348 and based on surface tension, pressure, and energy dissipation  
 349 forces because of friction were used to interpret the results.  
 350 From this study, the following conclusions could be extracted:

- 351 • Induction heating applies the heat directly into the bitu-  
 352 men. Therefore, it is more efficient than infrared radi-  
 353 ation and the healing times are much shorter.

**FIG. 10** Master curves of bitumen recovered from samples subjected to infrared radiation over different periods of time.



- When applying infrared radiation, the temperature increased only until steady-state temperature (approximately 100°C) was reached. However, with induction heating, the temperature never stopped increasing with the heating time, reaching temperatures close to the flash-point of bitumen.
- Both methods produced similar and satisfactory healing ratios up to 90 %. However, the induction heating needed significantly less energy for self-healing.
- There is an optimal infrared radiation energy for asphalt self-healing. Once this value is exceeded, further infrared radiation damages the material. This explains why cracks that develop in roads of very warm and sunny environments do not heal during the warm seasons.
- With infrared heating, the healing level of cracks increases when they are subjected to increasing differential temperatures. However, new damage is produced when they are subjected to steady temperatures for long time periods. Because a steady-state temperature was not reached when using induction heating, the healing ratios never stopped increasing.
- The aging of the bitumen during the heating process did not result in a feasible explanation for this behavior. Based on the theoretical background considered for the present research, there must be at least another factor, different from surface tension, hydrostatic forces and energy dissipation because of friction that affects asphalt self-healing in a significant way.

### ACKNOWLEDGMENTS

The writers acknowledge that the research leading to these results has received funding from the UK project EPSRC EP/M014134/1, “Induction Heating for Closing Cracks in Asphalt Concrete” and Infracation (an ERA-NET Plus on Infrastructure Innovation) under Grant No. 31109806.0003 - HEALROAD. Funding partners of the Infracation 2014 Call are: Ministerie van Infrastructuur en Milieu, Rijkswaterstaat, Bundesministerium für Verkehr, Bau und Stadtentwicklung, Danish Road Directorate, Statens Vegvesen Vegdirektoratet, Trafickverket-TRV, Vegagerdin, Ministere de l’Ecologie du Developpement Durable et de l’Energie, Centro para el Desarrollo Tecnológico Industrial, Anas S.P.S, Netivei Israel - National Transport Infrastructure Company, and Federal Highway Administration USDOT. The HEALROAD project is being carried out by the University of Cantabria, University of Nottingham, German Federal Highways Research Institute (BAST), European Union Road Federation (ERF), Heijmans Integrale projecten B.V., and SGS INTRON B.V.

### References

[1] Read, J. and Whiteoak, D., *The Shell Bitumen Handbook*, Thomas Telford, London, 2003.



AQ6

- 402 [2] Garcia, A., Bueno, M., Norambuena-Contreras, J.,  
403 and Partl, M. N., "Induction Healing of Dense  
404 Asphalt Concrete," *Constr. Build. Mater.*, Vol. 49, 2013,  
405 pp. 1–7, <http://dx.doi.org/10.1016/j.conbuildmat.2013.07.105>
- 406 [3] Menozzi, A., Garcia, A., Partl, M. N., Tebaldi, G., and  
407 Schuetz, P., "Induction Healing of Fatigue Damage in  
408 Asphalt Test Samples," *Constr. Build. Mater.*, Vol. 74,  
409 2015, pp. 162–168, <http://dx.doi.org/10.1016/j.conbuildmat.2014.10.034>
- 410 [4] Garcia, A., Bueno, M., Norambuena-Contreras, J., and  
411 Partl, M. N., "Single and Multiple Healing of Porous and  
412 Dense Asphalt Concrete," *J. Intell. Mater. Syst. Struct.*,  
413 Vol. 26, No. 4, 2015, pp. 425–433, <http://dx.doi.org/10.1177/1045389X14529029>
- 414 [5] Dai, Q., Wang, Z., and Mohd Hasan, M. R., "Investigation  
415 of Induction Healing Effects on Electrically Conductive  
416 Asphalt Mastic and Asphalt Concrete Beams Through  
417 Fracture-Healing Tests," *Constr. Build. Mater.*, Vol. 49,  
418 2013, pp. 729–737, <http://dx.doi.org/10.1016/j.conbuildmat.2013.08.089>
- 419 [6] Ayar, P., Moreno-Navarro, F., and Rubio-Gamez, M. C.,  
420 "The Healing Capability of Asphalt Pavements: A State of  
421 the Art Review," *J. Clean. Prod.*, Vol. 113, 2016, pp. 28–40,  
422 <http://dx.doi.org/10.1016/j.jclepro.2015.12.034>
- 423 [7] Garcia, A., Schlangen, E., and van de Ven, M., "Two Ways  
424 of Closing Cracks on Asphalt Concrete Pavements: Micro-  
425 capsules and Induction Heating," *Key Eng. Mater.*, Vols.  
426 417–418, 2010, pp. 573–576.
- 427 [8] Garcia, A., Bueno, M., Norambuena-Contreras, J., Partl,  
428 M. N., and Schuetz, P., "Uniformity and Mechanical Prop-  
429 erties of Dense Asphalt Concrete With Steel Wool Fibres,"  
430 *Constr. Build. Mater.*, Vol. 43, 2013, pp. 107–117, <http://dx.doi.org/10.1016/j.conbuildmat.2013.01.030>
- 431 [9] Apostolidis, P., Liu, X., Scarpas, A., Kasbergen, C., and van  
432 de Ven, M. F. C., "Advanced Evaluation of Asphalt Mortar  
433 for Induction Healing Purposes," *Constr. Build. Mater.*,  
434 Vol. 126, 2016, pp. 9–25, <http://dx.doi.org/10.1016/j.conbuildmat.2016.09.011>
- 435 [10] Liu, Q., Garcia, A., Schlangen, E., and van de Ven, M.,  
436 "Induction Healing of Asphalt Mastic and Porous Asphalt  
437 Concrete," *Constr. Build. Mater.*, Vol. 25, No. 9, 2011,  
438 pp. 3746–3752, <http://dx.doi.org/10.1016/j.conbuildmat.2011.04.016>
- 439 [11] Garcia, A., "Self-Healing of Open Cracks in Asphalt  
440 Mastic," *Fuel*, Vol. 93, 2012, pp. 264–272, <http://dx.doi.org/10.1016/j.fuel.2011.09.009>
- 441 [12] Garcia, A., Schlangen, E., van de Ven, M., and Liu, Q., "A  
442 Simple Model to Define Induction Heating in Asphalt  
443 Mastic," *Constr. Build. Mater.*, Vol. 31, 2012, pp. 38–46,  
444 <http://dx.doi.org/10.1016/j.conbuildmat.2011.12.046>
- 445 [13] Pauli, A. T., "Chemomechanics of Damage Accumulation  
446 and Damage-Recovery Healing in Bituminous Asphalt  
447 Binders," Ph.D. thesis, TU Delft, Delft, Netherlands, 2014.
- 448 [14] Qiu, J., "Self-Healing of Asphalt Mixtures, Towards a  
449 Better Understanding," Ph.D. thesis, TU Delft, Delft,  
450 Netherlands, 2012.
- 451 [15] Apeageyi, A. K., Grenfell, J. R. A., and Airey, G. D.,  
452 "Observation of Reversible Moisture Damage in Asphalt  
453 Mixtures," *Constr. Build. Mater.*, Vol. 60, 2014, pp. 73–80,  
454 <http://dx.doi.org/10.1016/j.conbuildmat.2014.02.033>
- 455 [16] Garcia, A., Schlangen, E., van de Ven, M., and van Vliet,  
456 D., "Induction Heating of Mastic Containing Conductive  
457 Fibers and Fillers," *Mater. Struct.*, Vol. 44, No. 2, 2011,  
458 pp. 499–508, <http://dx.doi.org/10.1617/s11527-010-9644-2>
- 459 [17] Ongel, A. and Harvey, J. T., "Analysis of 30 Years of Pave-  
460 ment Temperatures Using the Enhanced Integrated Cli-  
461 mate Model (EICM)," *UCPRC-RR-2004/05*, Pavement  
462 Research Center, Institute of Transportation Studies, Uni-  
463 versity of California Berkeley, University of California  
464 Davis, Berkeley/Davis, CA.
- 465 [18] Gómez-Meijide, B., Ajam, H., Lastra-González, P., and  
466 Garcia, A., "Effect of Air Voids Content on Asphalt Self-  
467 Healing via Induction and Infrared Heating," *Constr.*  
468 *Build. Mater.*, Vol. 126, 2016, pp. 957–966, <http://dx.doi.org/10.1016/j.conbuildmat.2016.09.115>
- 469 [19] National Center for Asphalt Technology at Auburn Uni-  
470 versity (NCAT), "Hot Mix Asphalt Materials," *Mixture*  
471 *Design and Construction*, 3rd ed., Lanham, MD, 2009.
- 472 [20] Witczak, M. W. and Bari, J., "Development of a Master  
473 Curve ( $E^*$ ) Database for Lime Modified Asphaltic  
474 Mixtures," *Research Project*, Arizona State University,  
475 Tempe, AZ, 2004.
- 476 [21] Heyes, D. M., Mitchell, P. J., and Visscher, P. B.,  
477 "Viscoelasticity and Near-Newtonian Behaviour of  
478 Concentrated Dispersions by Brownian Dynamics  
479 Simulations," *Trends Colloid Interf. Sci.*, Vol. 97, 1994,  
480 pp. 179–182, <http://dx.doi.org/10.1007/bfb0115161>
- 481 [22] Sung, Y. T., Kum, C. K., Lee, H. S., Kim, J. S., Yoon, H. G.,  
482 and Kim, W. N., "Effects of Crystallinity and Crosslinking  
483 on the Thermal and Rheological Properties of Ethylene  
484 Vinyl Acetate Copolymer," *Polymer*, Vol. 46, No. 25,  
485 2005, pp. 11844–11848, <http://dx.doi.org/10.1016/j.polymer.2005.09.080>